

# Suppression of Osteoclastogenesis by *N,N*-Dimethyl-*D*-erythro-sphingosine: A Sphingosine Kinase Inhibition-Independent Action

Hyung Joon Kim, Youngkyun Lee, Eun-Ju Chang, Hyun-Man Kim, Sam-Pyo Hong, Zang Hee Lee, Jiyeon Ryu, and Hong-Hee Kim

Department of Cell and Developmental Biology and BK21 Program (H.J.K., Y.L., E.-J.C., H.-M.K., Z.H.L., J.R., H.-H.K.); and Department of Oral Pathology and DRI (S.-P.H.), School of Dentistry, Seoul National University, Seoul, Korea

Received January 15, 2007; accepted May 15, 2007

## ABSTRACT

*N,N*-Dimethyl-*D*-erythro-sphingosine (DMS) competitively inhibits sphingosine kinase (SPHK) and has been widely used to assess the role of SPHK during cellular events, including motility, proliferation, and differentiation. In the present study, the effect of DMS on the differentiation of bone marrow macrophages (BMMs) to osteoclasts was investigated. When the osteoclast precursor cells were treated with DMS, the receptor activator of nuclear factor  $\kappa$ B ligand (RANKL)-induced osteoclastogenesis was completely blocked. We were surprised to find, however, that knock-down of SPHK by small interfering RNA (siRNA) in BMMs did not reduce osteoclastogenesis. Furthermore, both overexpression of SPHK and exogenous addition of sphingosine-1-phosphate, the product of SPHK activity, failed to overcome the antiosteoclastogenic effect of DMS. These results suggest that DMS inhibited osteoclastogenesis independently of SPHK. Subsequent characterization of the

DMS-mediated suppression of osteoclastogenesis revealed that DMS did not affect RANKL-induced activation of JNK, p38, NF- $\kappa$ B, and  $\text{Ca}^{2+}$  oscillation. On the other hand, DMS strongly inhibited two separate signaling pathways, the RANKL-induced activation of ERK and Akt, which eventually converged on the transcription factors c-Fos and NFATc1. There was significant increase in the osteoclast formation in the presence of DMS when BMMs were overexpressed with c-Fos, suggesting that c-Fos was a critical downstream target of DMS for the inhibition of osteoclastogenesis. Taken together, our data demonstrate that DMS has an antiosteoclastogenic function independently of its SPHK inhibitory activity. Considering previously reported anticancer properties of DMS, our study may also propose that DMS is an ideal drug candidate for bone metastases, for which osteoclastic bone-resorption is crucial.

Bone is a complex tissue composed of several cell types. The functions of bone are accomplished by continuous tissue renewal, termed "bone remodeling," occurring throughout life in the adult skeleton. The two major cell types responsible for bone remodeling are osteoclasts and osteoblasts. The

harmony between osteoclastic bone resorption and osteoblastic bone formation maintains skeletal homeostasis in adults (Walsh et al., 2006). In pathological bone resorption, this balance is tipped in favor of osteoclast formation, as seen in postmenopausal osteoporosis, autoimmune arthritis, periodontitis, and Paget's disease. Osteoclasts, the only type of cells responsible for bone resorption, are highly specialized cells originating from monocyte/macrophage lineage precursors. The single most important cytokine in the development of osteoclasts is receptor activator of nuclear factor  $\kappa$ B ligand (RANKL), whereas macrophage-colony stimulating factor (M-CSF), secreted by osteoblasts, provides the survival sig-

This work was supported by the Molecular and Cellular BioDiscovery Research Program (M1-0311-00-0024) and the 21C Frontier Functional Proteomics Project Grant (FPR05C2-280) from the Korea Science and Engineering Foundation, the Ministry of Science and Technology, Korea.

Article, publication date, and citation information can be found at <http://molpharm.aspetjournals.org>.  
doi:10.1124/mol.107.034173.

**ABBREVIATIONS:** RANKL, receptor activator of nuclear factor  $\kappa$ B ligand; M-CSF, macrophage-colony stimulating factor; RANK, receptor activator of nuclear factor  $\kappa$ B; TNF, tumor necrosis factor; NF- $\kappa$ B, nuclear factor  $\kappa$ B; MAPK, mitogen-activated protein kinase; JNK, c-Jun-N-terminal kinase; ERK, extracellular signal-regulated kinase; AP-1, activator protein 1; NFATc1, nuclear factor of activated T cells (NFATc1); S1P, sphingosine-1-phosphate; SPHK, sphingosine kinase; DMS, *N,N*-dimethyl-*D*-erythro-sphingosine; MEK, mitogen-activated protein kinase kinase; PI3K, phosphatidylinositol 3-kinase; HA, hemagglutinin; U0126, 1,4-diamino-2,3-dicyano-1,4-bis(methylthio)butadiene; BMM, bone marrow macrophage;  $\alpha$ -MEM,  $\alpha$ -minimal essential medium; FBS, fetal bovine serum; TRAP, tartrate-resistant acid phosphatase; MNC, multinucleated cell; siRNA, small interfering RNA; DMEM, Dulbecco's modified Eagle's medium; AM, acetoxymethyl ester; PCR, polymerase chain reaction; LY294002, 2-(4-morpholinyl)-8-phenyl-4*H*-1-benzopyran-4-one; PKC, protein kinase C; I $\kappa$ B, inhibitor of nuclear factor- $\kappa$ B.

nal to the precursor and differentiating cells (Boyle et al., 2003).

RANKL, expressed by osteoblasts, stromal cells, and activated T cells, signals through its receptor RANK (receptor activator of nuclear factor  $\kappa$ B), present on osteoclasts and their precursors (Boyle et al., 2003). Genetic experiments in mice have revealed that RANKL, RANK, tumor necrosis factor (TNF) receptor-associated factor 6, and the transcription factors c-Fos and nuclear factor  $\kappa$ B (NF- $\kappa$ B) are essential for precursors to commit into osteoclast lineage. The RANK signaling pathway can activate three major groups of mitogen-activated protein kinases (MAPKs): c-Jun N-terminal kinase (JNK), extracellular signal-regulated kinase (ERK), and p38. Association of TNF receptor-associated factor 6 with transforming growth factor- $\beta$ -activated kinase 1 activates JNK, AP-1, and NF- $\kappa$ B (Boyle et al., 2003; Lee et al., 2003; Huang et al., 2006). The transcription factor AP-1 is a heterodimeric protein composed of c-Fos proteins (c-Fos, Fos B, Fra-1, and Fra-2) and Jun proteins (c-Jun, Jun B, and Jun D). The activation of nuclear factor of activated T cells (NFATc1) has been found to be critical to osteoclast formation (Takayanagi et al., 2002). RANKL stimulates intracellular calcium oscillation, a requisite for calcineurin-mediated NFATc1 activation. NFATc1 then binds to its DNA response element via a ternary complex with AP-1 proteins, c-Fos/c-Jun, to transactivate osteoclastogenic genes (Takayanagi et al., 2002). It has been reported that NFATc1 expression is abolished in c-fos<sup>-/-</sup> precursors. Moreover, ectopically expressed NFATc1 could restore bone-resorbing activity in cells from c-fos<sup>-/-</sup> precursors in vitro and induce osteoclast differentiation in the absence of RANKL (Takayanagi et al., 2002; Matsuo et al., 2004). These findings have suggested that NFATc1 is both a key downstream target and a partner of c-Fos for efficient osteoclast differentiation.

Sphingolipids are ubiquitous membrane constituents of all eukaryotic cells. Intensive investigation in the past decade has established that sphingolipids, in addition to being structural components of cell membranes, play key roles as signaling molecules. In particular, three of these sphingolipid metabolites [ceramide, sphingosine, and sphingosine-1-phosphate (S1P)] have recently proved to be a new class of lipid messengers that regulate cell proliferation, migration, survival, and differentiation (Spiegel and Milstien 2003). The balance of these three lipid-signaling molecules is fine-tuned by sphingosine kinase (SPHK), which is a key enzyme catalyzing the formation of S1P by phosphorylating sphingosine, in response to diverse stimuli. Two mammalian isozymes, SPHK1 and SPHK2, have been cloned and characterized (Kohama et al., 1998). Several studies have demonstrated that SPHK can be activated by diverse stimuli, such as platelet-derived growth factor (Olivera and Spiegel 1993), TNF- $\alpha$  (Xia et al., 1999), vascular endothelial growth factor (Shu et al., 2002), and lipopolysaccharide (Wu et al., 2004). However, the role of SPHK and S1P on osteoclastogenesis has not been studied. Based on our microarray data that showed increased SPHK1 expression in response to RANKL, we began to investigate the potential role of SPHK for osteoclastogenesis in primary osteoclast precursor cells. We observed a potent inhibition of RANKL-induced osteoclast differentiation by a specific SPHK inhibitor, *N,N*-dimethyl-D-erythro-sphingosine (DMS). It is noteworthy that this effect of DMS was found to be independent of its SPHK inhibitory

activity. In fact, suppression of the MEK/ERK and the phosphatidylinositol 3-kinase (PI3K)/Akt pathways, which converged on the expression of c-Fos and NFATc1, was responsible for the antiosteoclastogenic function of DMS. Our study reveals for the first time the osteoclastogenesis inhibitory effect of DMS and provides an example of SPHK-independent action of DMS.

## Materials and Methods

**Reagents.** DMS and S1P were purchased from BIOMOL Research Laboratories (Plymouth Meeting, PA). Antibodies against phospho-ERK, ERK, phospho-JNK, JNK, phospho-p38, p38, phospho-I $\kappa$ B, and I $\kappa$ B were obtained from Cell Signaling Technology (Danvers, MA). Anti-hemagglutinin (HA) antibody was purchased from Covance Research Products (Berkeley, CA). Anti-NFATc1 and anti-actin antibodies were purchased from Santa Cruz Biotechnology, Inc. (Santa Cruz, CA) and Sigma Aldrich (St. Louis, MO), respectively. Anti-c-Fos antibody was obtained from Upstate Biotechnology, Inc. (Charlottesville, VA). U0126 was from Calbiochem (La Jolla, CA) and ionomycin was purchased from Sigma Aldrich (St. Louis, MO). [ $\gamma$ -<sup>32</sup>P]ATP (3000 Ci/mmol) was purchased from GE Healthcare (Chalfont St. Giles, Buckinghamshire, UK).

**Preparation of Macrophages from Mouse Bone Marrow and in Vitro Osteoclastogenesis.** Bone marrow macrophages (BMMs) were generated as described previously (Ha et al., 2003; Huang et al., 2006). In brief, bone marrow cells collected from long bones of 5- to 6-week-old ICR mice were plated on 100-mm Petri dishes and cultured for 16 to 24 h in  $\alpha$ -MEM (WelGENE Inc., Daegu, Republic of Korea) supplemented with 10% fetal bovine serum (FBS) containing 5 ng/ml M-CSF in 5% CO<sub>2</sub> at 37°C. Adherent cells were discarded, and remaining nonadherent cells were cultured in the presence of 30 ng/ml M-CSF. After 3 days, adherent cells were used as BMMs after washing out the nonadherent cells, including lymphocytes. These osteoclast precursor cells were further cultured for 3 days in the osteoclastogenic medium (medium containing 30 ng/ml M-CSF and 200 ng/ml RANKL) to generate osteoclasts unless otherwise indicated. Three days later, cells were stained for tartrate-resistant acid phosphatase (TRAP). TRAP-positive multinucleated cells (TRAP<sup>+</sup> MNC;  $\geq 3$  nuclei) were counted as osteoclasts.

**Plasmid Construction.** The full-length human SPHK1 cDNA was amplified from HeLa cell mRNA using sense primer 5'-GAATTCATGGATCCAGCGGGCGGCCCGG-3' and antisense primer 5'-GTCGACTCATAAGGGCTCTTCTGGCGGTGG-3' and cloned into pSra-HA vector. A retroviral vector, pMX-HA-SPHK1, was constructed by inserting a 1.4-kilobase fragment of human full-length SPHK1 cDNA. To generate retroviral vectors for siRNA experiments, targeting oligonucleotides were annealed and ligated into the pSuper-retro vectors (Oligoengine, Seattle, WA) using BamHI and HindIII sites. The sequences of used oligonucleotides are as follows: mouse SPHK1 siRNA, 5'-AGCTTAAAAATATGGAACCTTGACTGTCCATCTTGAATGGACAGTCAAGTTCCATAGGG-3' and 5'-GATCCCCTATGGAACCTTGACTGTCCATTCAAGAGATGGACAGTCAAGTTCCATATTTTAA-3'; mouse SPHK2 siRNA, 5'-GATCTCGATTGACCAATATGAGCAGCCTTGATATCCGGGCTGCTCATATTGGTCAATCTTTTTCCTCAA-3' and 5'-AGCTTTTGGAAAAAAGATTGACCAATATGAGCAGCCCGGATATCAAGGCTGCTCATATTGGTCAATCGA-3'; and luciferase siRNA, 5'-GATCTGTATAATACACCGCTACTTGTATATCCGGTAGCGCGGTGTATTATACTTTTTCCTCAA-3' and 5'-AGCTTTTGGAAAAAAGTATAATACACCGCTACCGGATATCAAGTAGCGCGGTGTATTATACA-3'.

**Retroviral Gene Transfer.** Retrovirus packaging was performed by transfection of pMX-HA-SPHK1 and pSuper-retro-siRNA plasmids into Plat-E cells. Transfection procedure was carried out using Lipofectamine 2000 (Invitrogen, Carlsbad, CA) according to the manufacturer's instructions. After incubation at 37°C for 6 h, the DNA mixture was replaced with DMEM supplemented with 10%

FBS. In the next day, the medium was changed with  $\alpha$ -MEM/10% FBS, and cells were further cultured for 48 h. Cell culture medium containing viral particles was collected and filtered with 0.45- $\mu$ m syringe filter (Sartorius AG, Goettingen, Germany). The filtered medium was stored at  $-70^{\circ}\text{C}$  until use. For infection with retroviruses, BMMs plated in six-well plates ( $1 \times 10^6$  cells/well) were incubated with the virus-containing medium (2 ml/well), Polybrene (10  $\mu\text{g/ml}$ ; Sigma), and M-CSF (30 ng/ml) for 1 day. A portion of infected cells was assayed for infection efficiency, and the rest of the cells were further cultured in osteoclastogenic medium (30 ng/ml M-CSF plus 200 ng/ml RANKL). After 3 days, osteoclastogenesis was evaluated by TRAP staining.

**Luciferase Reporter Assays.** Raw264.7 cells were plated at  $5 \times 10^5$  cells/well in six-well plates. The next day, cells were transfected with 4  $\mu\text{g}$  of NF- $\kappa$ B or NFATc1-dependent luciferase reporter vector using 10  $\mu\text{l}$  of Lipofectamine 2000 (Invitrogen) in DMEM. At 4 h after transfection, the medium was replaced by DMEM/10% FBS. After incubation for 14 h at  $37^{\circ}\text{C}$  in 5%  $\text{CO}_2$ , cells were collected by scraping, resuspended in  $\alpha$ -MEM/10% FBS, and replated in 96-well plates at  $2 \times 10^4$  cells/well. Cells were stimulated with 200 ng/ml RANKL in the presence or absence of DMS for 8 h. Cells were lysed in Reporter Lysis Buffer (Promega, Madison, WI), and luciferase activity was measured using a luminometer. The protein concentration of the cell lysates was also determined and the relative reporter activity per microgram of protein was calculated.

**Fluorescence Measurement of  $[\text{Ca}^{2+}]_i$ .** Intracellular calcium concentration ( $[\text{Ca}^{2+}]_i$ ) was measured using the fluorescent dye Fura-2/AM (Invitrogen). BMMs on noncoated glass coverslips were incubated with 30 ng/ml M-CSF and 200 ng/ml RANKL for 48 h in the presence or absence of 2  $\mu\text{M}$  DMS. To load the calcium indicator, the cells were incubated for 40 min at room temperature in culture medium containing 5  $\mu\text{M}$  Fura-2/AM and 0.05% Pluronic F127 (Invitrogen). After the incubation, cells were washed three times with Hank's balanced salt solution (Invitrogen). The cell ensembles were illuminated at wavelengths of 340 and 380 nm, and the emitted light, passed through a 510-nm interference filter, was detected with an intensifier charge-coupled device camera (International Ltd., Sterling, VA). Images were recorded at every 500 ms and analyzed using image analysis software (MetaFluor; Molecular Devices, Sunnyvale, CA).

**Immunoblotting.** Cells were disrupted in a lysis buffer (20 mM pH 7.4 Tris-HCl, 150 mM NaCl, 50 mM NaF, 2 mM sodium orthovanadate, 1 mM phenylmethylsulfonyl fluoride, 1  $\mu\text{g/ml}$  leupeptin, 1  $\mu\text{g/ml}$  aprotinin, 1  $\mu\text{g/ml}$  pepstatin, and 1% Triton X-100). Protein concentration of cell lysates was determined using the detergent-compatible protein assay kit (Bio-Rad Laboratories, Hercules, CA). For immunoblotting of NFATc1 and c-Fos, whole-cell extracts were prepared by disrupting cells with boiling sample buffer. Twenty to thirty micrograms of cell lysates or equal portions of whole-cell extracts were resolved by 8 to 10% SDS-polyacrylamide gel electrophoresis. Separated proteins were transferred to a polyvinylidene difluoride membrane (GE Healthcare). The membrane was blocked with 5% skim milk and probed with appropriate primary antibodies. After incubation with appropriate secondary antibodies, the immunoreactivity was detected with enhanced chemiluminescence reagents.

**Quantitative PCR Analysis.** Total RNAs were isolated with TRIzol reagent (Invitrogen), and 2  $\mu\text{g}$  of RNAs were reverse-transcribed with SuperScript II (Invitrogen) according to the manufacturer's instructions. For quantitative real-time PCR analysis, 4  $\mu\text{g}$  of cDNAs were amplified with SYBR green PCR master mix (Applied Biosystems, Warrington, Cheshire, UK) in a MicroAmp optical tube using AB7500 instrument (Applied Biosystems), for 40 cycles of 15 s of denaturation at  $95^{\circ}\text{C}$  and 1 min of amplification at  $60^{\circ}\text{C}$ . The PCR primer sequences were: SPHK1, 5'-CTGGTTCATGTGCCCGTGG-T-3' (forward) and 5'-CACTTGGCCCTGCACAGCTT-3' (reverse); Glyceraldehyde-3-phosphate dehydrogenase, 5'-AGGTCATCCCAG-AGCTGAACG-3' (forward) and 5'-CACCTGTTGCTGTAGCCGTA-

T-3' (reverse). Results were analyzed by 7500 system sequence detection software (ver. 1.3; Applied Biosystems) and the mRNA expression level of SPHK1 was normalized using the level of glyceraldehyde-3-phosphate dehydrogenase.

**Sphingosine Kinase Activity Assay.** Sphingosine kinase activity was measured as described previously (Ryu et al., 2006). In brief, Cells were scraped in SPHK assay buffer (20 mM Tris, pH 7.4, 20% glycerol, 1 mM mercaptoethanol, 1 mM EDTA, 1 mM sodium orthovanadate, 40 mM  $\beta$ -glycerophosphate, 15 mM NaF, 10  $\mu\text{g/ml}$  leupeptin, 10  $\mu\text{g/ml}$  aprotinin, 10  $\mu\text{g/ml}$  soybean trypsin inhibitor, 1 mM phenylmethylsulfonyl fluoride, and 0.5 mM 4-deoxyxypyridoxine) and disrupted by freeze-thawing. An 80- $\mu\text{g}$  portion of cell extracts in a 185- $\mu\text{l}$  volume was mixed with 5  $\mu\text{l}$  of  $[\gamma\text{-}^{32}\text{P}]\text{ATP}$  (5  $\mu\text{Ci}$ ) containing 0.2 M  $\text{MgCl}_2$  and 10  $\mu\text{l}$  of 1 mM sphingosine (dissolved in 5% Triton X-100) and then incubated for 30 min at  $37^{\circ}\text{C}$ . The reaction was terminated with 10  $\mu\text{l}$  of 1 N HCl. A 400- $\mu\text{l}$  portion of chloroform/methanol/HCl [100:200:1 (v/v)] mixture was added and mixed. Then, 120  $\mu\text{l}$  of chloroform and 120  $\mu\text{l}$  of 2 M KCl were added, and phases were separated by centrifugation. The organic phase was dried and resolved by thin-layer chromatography on silica gel G60 with SPHK1-butanol/methanol/acetic acid/water [80:20:10:20 (v/v)]. The radioactive spots corresponding to S1P were detected using filmless autoradiographic analysis (BAS-1500; Fujifilm Co. Ltd, Tokyo, Japan).

**Cytotoxicity Assay.** Cytotoxicity of DMS was evaluated with the Cell Counting Kit-8 (Dojindo Laboratories, Kumamoto, Japan). BMMs were plated in 96-well plates at a density of  $2 \times 10^4$  cells/well in triplicate and treated with increasing concentrations of DMS. After a 16-h incubation, 10  $\mu\text{l}$  of the solution of Cell Counting Kit-8 was added to each well, and the plate was incubated for an additional 2 h. The absorbance of each well was measured at 450 nm with a reference at 655 nm using Benchmark microplate reader (Bio-Rad Laboratories).

**Fluorescence Microscopy.** BMMs on noncoated glass coverslips were infected with pMX-GFP or pMX-GFP-c-Fos retroviruses. At 24 h after infection, cells were washed twice with ice-cold PBS and fixed with 3.7% formaldehyde. Coverslips were mounted on glass slides, and images were photographed under Zeiss AxioImager D.1 fluorescence microscope (Carl Zeiss Inc., Thornwood, NY).

## Results

**DMS Suppressed Osteoclastogenesis in Primary BMMs Cultured with RANKL and M-CSF.** In microarray experiments to investigate the changes in the gene expression profile during osteoclast differentiation, we found that the sphingosine kinase 1 (SPHK1) expression is increased in response to RANKL (data not shown). To confirm the SPHK1 up-regulation, we analyzed the mRNA levels of SPHK1 in mouse bone marrow-derived macrophages (BMMs), primary osteoclast precursor cells, by quantitative real-time polymerase chain reaction. Incubation of BMMs in the osteoclastogenic medium (containing RANKL plus M-CSF) increased the SPHK1 mRNA level (Fig. 1A, bottom). Elevation in the protein level of SPHK1 was also observed (Fig. 1A, top two panels). The SPHK1 up-regulation was not detected in medium containing only M-CSF (data not shown), indicating that RANKL was responsible for the SPHK1 induction. M-CSF was included in long-term cultures because BMMs fail to survive in the absence of this factor. SPHK2 mRNA and protein levels were also increased by RANKL (data not shown). The increase in SPHK1 expression by RANKL raised the possibility of involvement of this lipid kinase and its product, S1P, in osteoclast differentiation. To explore this possibility, we used DMS, a competitive inhibitor of SPHK.

BMMs were induced to differentiate by culturing in osteoclastogenic medium containing RANKL and M-CSF, and differentiated osteoclasts were identified by tartrate-resistant acid phosphatase (TRAP) staining. In the absence of RANKL, no TRAP-positive multinucleated cells (TRAP<sup>+</sup> MNC; osteoclasts) were generated (data not shown). Addition of DMS to the BMM culture in the presence of RANKL inhibited the formation of TRAP<sup>+</sup> MNC in a dose-dependent

manner (Fig. 1, B and C). No cytotoxicity of DMS was observed at the concentrations used (Fig. 1D), indicating that the antiosteoclastogenic effect of DMS was not due to toxic effects on the precursor cells to differentiate. At 1  $\mu$ M, DMS profoundly reduced SPHK activity (Fig. 1E). DMS also inhibited the osteoclast formation in RANKL-stimulated RAW264.7 cells, an established myeloid line of cells used in osteoclastogenesis studies (data not shown).

**DMS Suppression of Osteoclastogenesis Was Independent of SPHK.** Because DMS significantly inhibited the RANKL-induced osteoclastogenesis, we evaluated the role for SPHK in osteoclast differentiation by introducing siRNA targeted to SPHK1 and SPHK2 to BMMs by retroviral transduction (Fig. 2A). Contrary to our expectation, the reduction in SPHK1 and -2 expression by SPHK1/2-siRNA did not cause a decrease in osteoclast formation; rather, it significantly increased osteoclastogenesis (Fig. 2, B and E). These data raised the possibility that DMS might function in a manner independent of its SPHK inhibitory activity during RANKL-induced osteoclastogenesis. To further clarify the relationship between SPHK and antiosteoclastogenic effect of DMS, we overexpressed SPHK1 in BMMs by infecting with retroviruses harboring HA-tagged SPHK1. Overexpression of

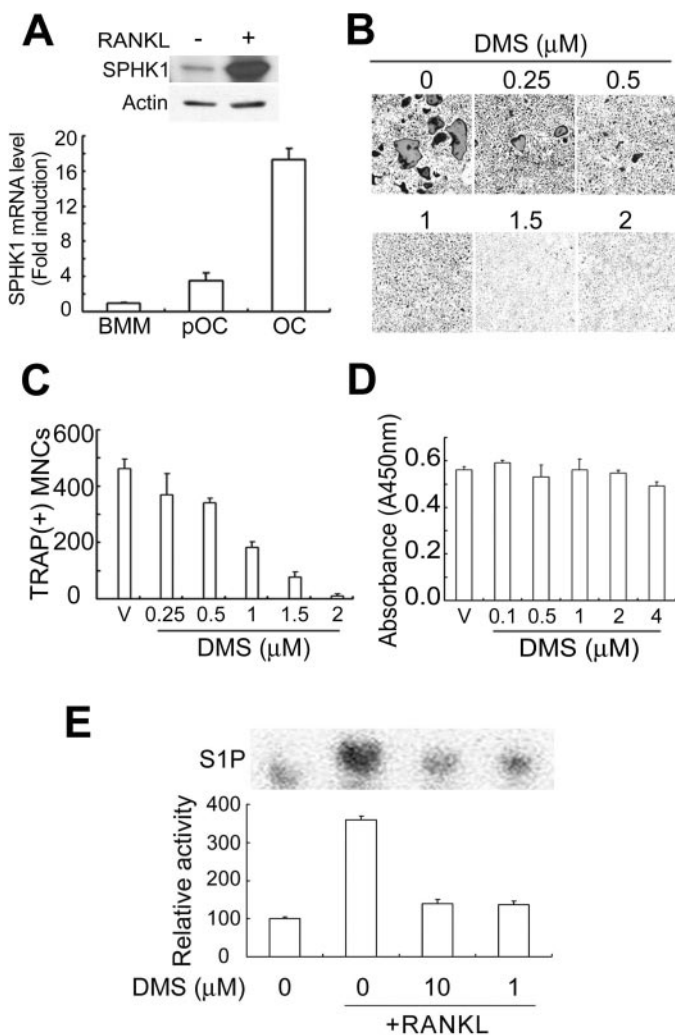


**Fig. 1.** DMS inhibited RANKL-induced osteoclastogenesis from primary precursor cells. A, mouse bone marrow-derived macrophages (BMMs) were incubated in the osteoclastogenic medium (containing 30 ng/ml M-CSF plus 200 ng/ml RANKL) or in medium containing only M-CSF (30 ng/ml) for 3 days. Cell lysates were prepared and the protein levels of SPHK1 and actin were examined by Western blotting (top two panels). In addition, SPHK1 mRNA expression at day 0 (BMM), day 2 (preosteoclast, pOC), or day 3 (osteoclast, OC) was analyzed by quantitative polymerase chain reaction. Results are presented as -fold induction of SPHK1 mRNA (bottom panel). B and C, BMMs were cultured in the osteoclastogenic medium for 3 days in the presence of DMS (0.25–2  $\mu$ M) or vehicle (V; DMSO). Cells were stained for TRAP and numbers of TRAP-positive multinuclear cells containing more than three nuclei (TRAP<sup>+</sup> MNC) were counted. D, BMMs were cultured in the osteoclastogenic medium for 24 h together with DMS (0.1–2  $\mu$ M) or vehicle (V). Cell viability was evaluated as described under *Materials and Methods*. E, BMMs were serum-starved for 5 h, pretreated with or without DMS (2  $\mu$ M) for 2 h, and stimulated with RANKL (500 ng/ml) for 15 min. After RANKL stimulation, SPHK activity was measured in cell extracts using [ $\gamma$ -<sup>32</sup>P]ATP and sphingosine. The reaction products were resolved by thin-layer chromatography and the radioactive spots corresponding to S1P were detected using filmless autoradiographic analysis.

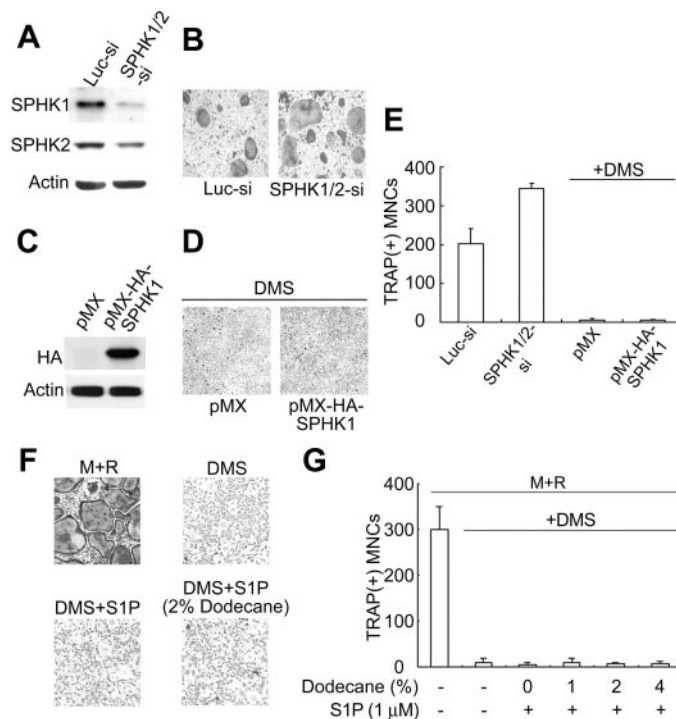


**Fig. 2.** SPHK knock-down and overexpression revealed an SPHK-independent effect of DMS on osteoclastogenesis. A and B, BMMs were infected with retroviruses harboring SPHK1 siRNA plus SPHK2 siRNA (SPHK1/2-si) or luciferase siRNA (Luc-si). Then, cells were cultured for 3 days in the osteoclastogenic medium. One of the duplicate cultures was lysed, and equal amounts of proteins (30  $\mu$ g) were immunoblotted with anti-SPHK1 or anti-SPHK2 antibody. The other set of cells was TRAP-stained. C and D, BMMs were infected with retroviruses for pMX or pMX-HA-SPHK1. Cells were cultured for 3 days in the osteoclastogenic medium in the presence of DMS (2  $\mu$ M). The overexpression of SPHK1 was confirmed by immunoblotting with anti-HA antibody, and the osteoclast differentiation was examined by TRAP staining. E, The number of TRAP<sup>+</sup> MNCs generated in B and D was scored. F and G, BMMs were cultured for 3 days in the osteoclastogenic medium with DMS (2  $\mu$ M) together with S1P dissolved in methanol or dissolved in methanol/dodecane mixture [used at 99:1–96:4 (v/v)]. Cells were stained for TRAP and the number of TRAP<sup>+</sup> MNCs was counted.

SPHK1 was confirmed by Western blotting with anti-HA antibody (Fig. 2C). When the osteoclastogenesis was evaluated from the SPHK1-overexpressing BMMs, DMS still potently suppressed the osteoclastogenesis (Fig. 2, D and E). This result further supports the SPHK-independent antiosteoclastogenic action of DMS.

SPHK catalyzes the phosphorylation of sphingosine, and resulting S1P works as a bioactive molecule (Spiegel and Milstien 2003). It has become clear that the biological role of extracellular S1P is mediated by plasma membrane S1P receptors (Olivera and Spiegel, 1993; Spiegel and Milstien, 2003). BMMs expressed four members of S1P receptors—EDG1/S1P<sub>1</sub>, EDG5/S1P<sub>2</sub>, EDG3/S1P<sub>3</sub>, and EDG8/S1P<sub>5</sub> (data not shown). To further confirm the SPHK-independent suppression of osteoclast formation by DMS, we treated BMMs with S1P. Exogenously added S1P (dissolved in methanol) could not rescue the DMS suppression of osteoclast formation even at doses as high as 10  $\mu$ M (data not shown). The methanol/dodecane mixture, which facilitates intracellular delivery of sphingolipids, has been described previously (Tauzin et al., 2007). Therefore, we used a dodecane delivery of S1P into the cells to elucidate whether S1P needs to be transported across the plasma membrane in osteoclastogenesis (Fig. 2, F and G). However, exogenously added S1P, dissolved in methanol/dodecane mixture, also failed to reverse the antiosteoclastogenic effect of DMS. The S1P concentrations used were not cytotoxic to BMMs (data not shown). Taken together, these data demonstrate that the antiosteoclastogenic effect of DMS might be independent of SPHK.

**DMS Had No Effect on RANKL-Induced NF- $\kappa$ B Activation.** The SPHK-independent mode of DMS activity for osteoclastogenesis suppression led us to investigate the effects of this inhibitor on the activation of transcription factors and signaling molecules that have been reported to be crucial for osteoclast differentiation. NF- $\kappa$ B activation composes an essential part of osteoclastogenic signaling pathways by stimulating induction of several osteoclastogenesis-associated genes, such as TRAP, cathepsin K, and MMP9 (Boyle et al., 2003; Lee and Kim, 2003). Furthermore, it has recently been reported that NF- $\kappa$ B regulates the expression of NFATc1, another key transcription factor for osteoclastogenesis (Takatsuna et al., 2005). In general, NF $\kappa$ B activation starts from phosphorylation and subsequent degradation of the inhibitory subunit I $\kappa$ B in response to an extracellular signal. The freed NF $\kappa$ B then translocates to the nucleus to bind target gene promoters. To examine whether NF $\kappa$ B could be a target of DMS during the suppression of osteoclastogenesis, we stimulated BMMs with RANKL in the presence or absence of DMS and assessed the activation of NF- $\kappa$ B. DMS did not affect the RANKL-induced phosphorylation and subsequent degradation of I $\kappa$ B (Fig. 3A). A promoter activity reporter assay for NF- $\kappa$ B consistently revealed no effect of DMS on the RANKL-induced NF- $\kappa$ B activity (Fig. 3B). Therefore, NF $\kappa$ B is not the target of DMS for its inhibition of RANKL-induced osteoclastogenesis.

**DMS Blocks the Expression of NFATc1 Induced by RANKL in BMMs.** It has been shown by several reports that the NFATc1 transcription factor is greatly up-regulated by RANKL, and its induction is critical to efficient osteoclast differentiation (Takayanagi et al., 2002; Walsh et al., 2006). To explore the potential effect of DMS on NFATc1 induction by RANKL, we treated BMMs with the osteoclastogenic me-

dium (M-CSF plus RANKL) together with or without DMS for various time periods, and assessed the NFATc1 expression. The induction of NFATc1 protein level was clearly observed at 12 h, and even higher levels of NFATc1 were detected at 24~72 h (Fig. 4A). This elevation in NFATc1 expression was not detected in the absence of RANKL (Fig. 4B, lane M). DMS treatment strongly reduced the induction of NFATc1 by RANKL in BMMs (Fig. 4A). The inhibition of RANKL induction of NFATc1 by DMS was dose-dependent (Fig. 4B). In line with the inhibitory effect on NFATc1 protein level, DMS treatment decreased NFATc1-dependent reporter activity in response to RANKL stimulation (Fig. 4C).

**DMS Did Not Inhibit RANKL-Induced Ca<sup>2+</sup> Oscillation in BMMs.** It has been reported that the sustained Ca<sup>2+</sup> oscillation induced by RANKL is essential for the autoamplification of NFATc1 gene expression, which is critical to NFATc1-dependent osteoclastogenic gene transcription (Takayanagi et al., 2002). Because DMS inhibited the NFATc1 induction by RANKL, we next explored the potential involvement of Ca<sup>2+</sup> oscillation response in the antiosteoclastogenic function of DMS. The intracellular Ca<sup>2+</sup> levels were determined in BMMs cultured in the osteoclastogenic medium with or without DMS (Fig. 4D). Upon gross examination, we found that DMS did not alter the cell population showing Ca<sup>2+</sup> oscillation (approximately 20~30%; data not shown) and the frequency of Ca<sup>2+</sup> spikes in RANKL-treated cells. Although it slightly decreased oscillation amplitude, it is likely that DMS did not block RANKL-induced Ca<sup>2+</sup> oscillation.

**DMS Inhibits c-Fos Expression in RANKL-Stimulated BMMs.** Another important factor in NFATc1 induction by RANKL in osteoclast precursor cells is c-Fos. It has been

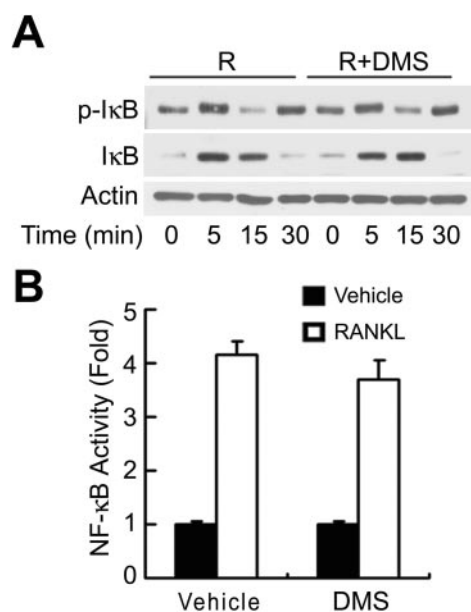


**Fig. 3.** DMS had no effect on RANKL-induced NF $\kappa$ B activation. A, BMMs were serum-starved for 5 h, pretreated with or without DMS (2  $\mu$ M) for 2 h, and stimulated with RANKL (500 ng/ml) for the indicated times. Cells were lysed and subjected to immunoblotting with an antibody for p-I $\kappa$ B or I $\kappa$ B. B, Raw264.7 cells were transfected with an NF $\kappa$ B reporter luciferase plasmid. At 14 h after transfection, cells were serum-starved for 5 h, pretreated with or without DMS (2  $\mu$ M) for 2 h, and stimulated with RANKL (200 ng/ml) for 24 h. Cells were lysed and the luciferase activity was determined. The relative NF $\kappa$ B activity was presented by luciferase activity per microgram of protein.

reported that expression of NFATc1 is induced in *c-Fos*<sup>+/+</sup> mice, but not in *c-fos*<sup>-/-</sup> mice during osteoclast differentiation (Takayanagi et al., 2002; Matsuo and Ray, 2004; Matsuo et al., 2004). As a component of the AP-1 transcription factor, *c-Fos* was suggested to regulate the NFATc1 induction by RANKL (Takayanagi et al., 2002; Matsuo and Ray, 2004; Matsuo et al., 2004). We therefore examined whether DMS could interfere with the *c-Fos* regulation by RANKL. BMMs were incubated in RANKL together with either DMS or vehicle and analyzed *c-Fos* expression levels. The *c-Fos* protein started to slightly increase from 30 min after stimulation and reached to a greatly elevated level from 6 h (Fig. 5A). DMS

strongly inhibited the RANKL induction of *c-Fos* protein (Fig. 5A). The inhibitory effect of DMS was also observed in cells stimulated for up to 3 days (Fig. 5B). In BMMs treated with various concentrations of DMS, dose dependence of the inhibition was observed (Fig. 5C). It is noteworthy that the induction of *c-Fos* occurred faster than that of NFATc1 (Figs. 4A and 5A). This observation is congruent with the current understanding that *c-Fos* plays a critical role for NFATc1 induction. Thus, the decreased level of *c-Fos* may explain the ablation of NFATc1 induction by DMS. Together with data shown in Fig. 4D, It could be concluded that DMS blocks the induction of NFATc1 by interfering with the RANKL signaling for *c-Fos* expression, but not that for Ca<sup>2+</sup> oscillation.

**DMS Inhibits the Activation of ERK, but Not That of JNK and p38 MAPKs by RANKL in BMMs.** The activation of MAPK signaling pathways by RANKL is an important mechanism involved in osteoclastogenesis (Lee and Kim, 2003; Teitelbaum, 2004). The activation of ERK, JNK, and p38 MAPKs by RANKL and their contribution to osteoclastogenesis has been demonstrated with pharmacological inhibitors and dominant-negative forms (Matsumoto et al., 2000; Wei et al., 2002). In addition, ERK has been well documented to induce and activate *c-Fos* (Treisman, 1996; Müller et al., 1997). Therefore, we next focused on the effect of DMS on the activation of ERK and the other two MAPK family member proteins. When the MAPK activity was assessed by Western blotting with phosphorylated form-specific antibodies, it was found that DMS strongly suppressed the activation of ERK by RANKL in BMMs (Fig. 6A). In contrast, the RANKL-stimulated activation of JNK and p38 was not affected by DMS (Fig. 6, B and C). Therefore, it is possible that DMS suppressed *c-Fos* and NFATc1 induction by inhibiting the ERK activation by RANKL, resulting in a blockade in osteoclastogenesis.

**DMS Suppresses the Activation of MEK by RANKL in BMMs.** The activation of ERK occurs through phosphorylation of both threonine and tyrosine residues by upstream MAP kinase kinases, MEK1/2 (Payne et al., 1991). The activation of MEK1/2 occurs through phosphorylation of two serine residues by Raf-like molecules (Pearson et al., 2001).

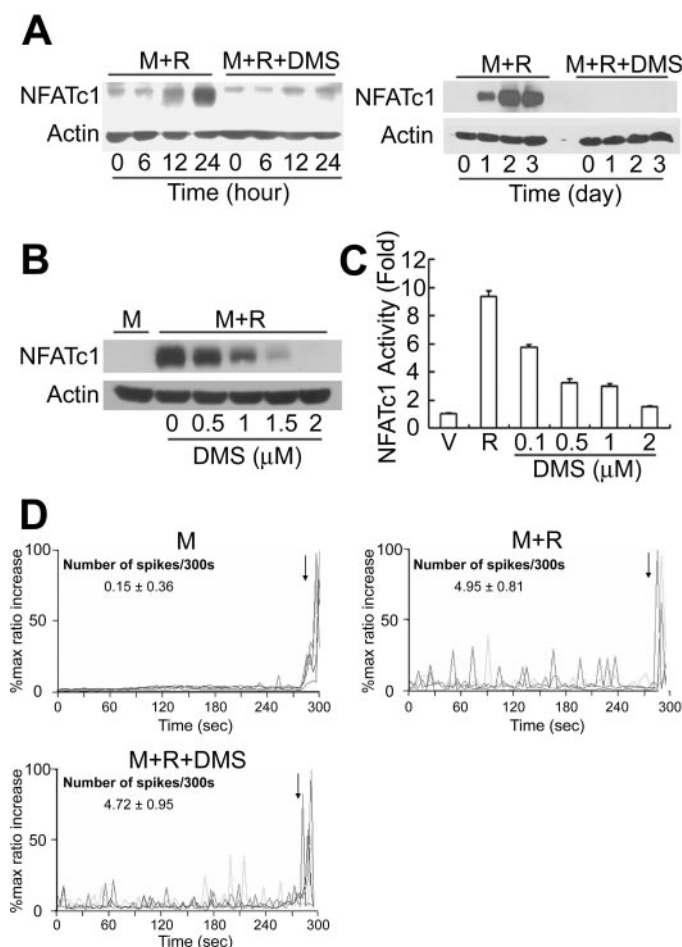


**Fig. 4.** DMS blocked the expression of NFATc1 induced by RANKL in BMMs. A, BMMs were cultured in the osteoclastogenic medium (M+R; 30 ng/ml M-CSF + 200 ng/ml RANKL) for the indicated hours (left) and days (right) in the absence or presence of DMS (2  $\mu$ M). NFATc1 expression was determined by immunoblotting with an anti-NFATc1 antibody. B, BMMs were cultured in the osteoclastogenic medium (M+R) or medium containing M-CSF (M) for 24 h with or without DMS (0.5–2  $\mu$ M). NFATc1 expression was determined by immunoblotting with an anti-NFATc1 antibody. C, Raw264.7 cells were transfected with an NFATc1 reporter luciferase plasmid. At 14 h after transfection, cells were stimulated with 200 ng/ml RANKL together with indicated concentrations of DMS or vehicle (DMSO) for 24 h. Cells were lysed and the luciferase activity was determined. The relative NFATc1 activity was presented by luciferase activity per microgram of protein. D, BMMs on glass coverslips were grown in the medium containing M-CSF (M) or M-CSF+RANKL (M+R) for 48 h in the presence or absence of DMS (2  $\mu$ M). Cells were loaded with Fura-2/AM (5  $\mu$ M), and imaging was performed as described under *Materials and Methods*. Maximum ratio increase was obtained with the addition of 10  $\mu$ M ionomycin at the end of each experiment. Each color indicates individual cell in the same field, and black color indicates the baseline status.

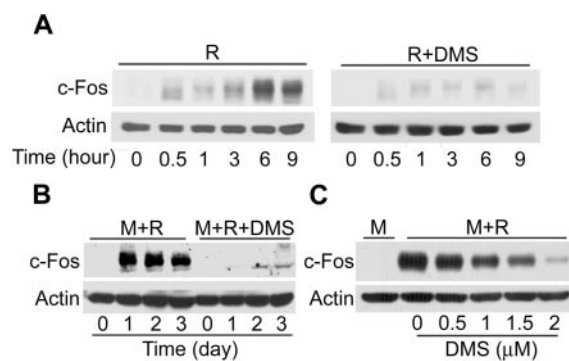


**Fig. 5.** DMS blocked *c-Fos* induction by RANKL in BMMs. A, BMMs were incubated with 200 ng/ml RANKL for the indicated hours in the absence or presence of DMS (2  $\mu$ M). The *c-Fos* expression was determined by immunoblotting with an anti-*c-Fos* antibody. B, BMMs were cultured in the osteoclastogenic medium (M+R) for the indicated days with or without DMS (2  $\mu$ M). M-CSF was included in long-term cultures because BMMs fail to survive in the absence of this factor. The *c-Fos* expression was analyzed by immunoblotting. C, BMMs were cultured in the medium containing M-CSF (30 ng/ml) or M-CSF plus RANKL (200 ng/ml) for 24 h in the presence or absence of DMS (0.5–2  $\mu$ M). *c-Fos* expression was determined by immunoblotting.

Because DMS inhibited ERK activation by RANKL, we next investigated the activation of the upstream kinase MEK1/2 by RANKL and effects of DMS on MEK1/2 activity. As shown in Fig. 7A, DMS greatly reduced MEK1/2 phosphorylation in response to RANKL in BMMs. Therefore, the MEK-ERK pathway to c-Fos induction is likely to be the target in the DMS-mediated antiosteoclastogenesis effect. Therefore, we next explored the relationship between the MEK/ERK pathway, osteoclast differentiation, and the osteoclastogenic transcription factors c-Fos and NFATc1. For this investigation, U0126, a specific MEK inhibitor, was used, and its effects on osteoclastogenesis and the induction of c-Fos and NFATc1 were evaluated. U0126 blocked the activation of ERK1/2 at concentrations 0.1 to 10  $\mu\text{M}$  (Fig. 7B). When BMMs were cultured in the osteoclastogenic medium in the presence of U0126, osteoclast formation was profoundly suppressed (Fig. 7, C and D). Consistent with its osteoclastogenesis-inhibitory effect, U0126 inhibited the induction of c-Fos by RANKL in BMMs (Fig. 7E, top panel). Likewise, the induction of NFATc1 by RANKL was suppressed by U0126 in a dose-dependent manner (Fig. 7E, third panel).

**DMS Inhibited PI3K and MEK1/2 Activation Independently.** The PI3K/Akt pathway is also an important component of RANKL signaling in osteoclast precursor cells (Wong et al., 1999). It is noteworthy that DMS has been documented to impede the PI3K/Akt signaling pathway in epithelial cells (Monick et al., 2004). On the other hand, PI3K has been shown to stimulate ERK1/2 activation in response

to TNF- $\alpha$ , insulin, and nerve growth factor (Grønning et al., 2002; Zhuang et al., 2004; Lee et al., 2005). With these previous findings, we wondered whether DMS would affect the PI3K/Akt activation by RANKL in BMMs and, if it did, whether the PI3K/Akt inhibition was related to the DMS-mediated suppression of MEK-ERK activation by RANKL. When the activation of Akt was examined by Western blotting with antiphospho-Akt, Akt activation by RANKL was detected from 8 min after stimulation in BMMs (Fig. 8A, lanes 1–5). This Akt activation was greatly inhibited in the presence of DMS (Fig. 8A, lanes 6–9). Next, we investigated whether the Akt inhibition mediates the DMS-induced suppression of ERK activation by RANKL. BMMs were treated with the PI3K inhibitor LY294002 to block Akt activation, and the phosphorylation of ERK in response to RANKL was assessed. As shown in Fig. 7B, LY294002 abolished Akt activation by RANKL (Fig. 8B, top). However, the ERK1/2

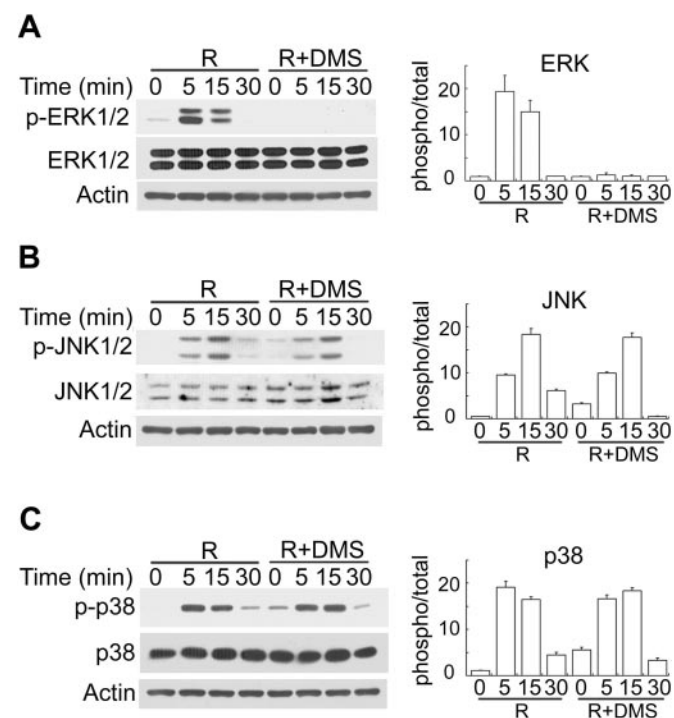


**Fig. 6.** DMS inhibited RANKL-induced ERK activation. BMMs were serum-starved for 5 h, pretreated with or without DMS (2  $\mu\text{M}$ ) for 2 h, and stimulated with RANKL (500 ng/ml) for the indicated times. The phosphorylated forms of ERK1/2 (A), JNK1/2 (B) and p38 (C) were detected with phosphospecific antibodies. Blots were stripped and reprobed with the control antibodies to demonstrate comparable loading. Protein band intensities were quantified by densitometry, and the levels of phosphorylated MAPKs were normalized to the total levels of corresponding MAPKs. The ratio of phospho/total MAPKs in the RANKL-stimulated cells was compared with that of untreated cells.

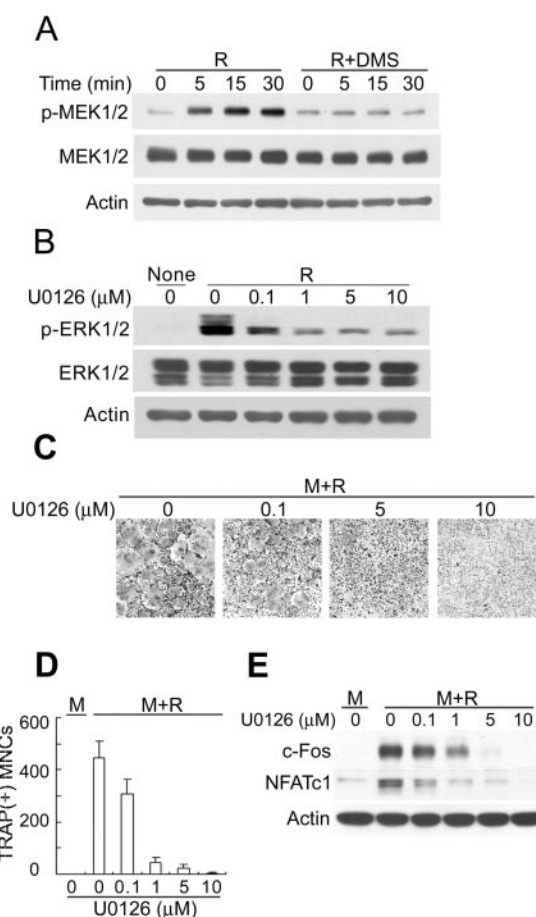


**Fig. 7.** Inhibition of RANKL-induced MEK activation mediates the anti-osteoclastogenic effect of DMS. A, BMMs were serum-starved for 5 h, pretreated with or without DMS (2  $\mu\text{M}$ ) for 2 h, and stimulated with RANKL (500 ng/ml) for the indicated times. Cell lysates were analyzed by immunoblotting with a phospho-MEK1/2 antibody. The same blot was stripped and reprobed with an anti-MEK1/2 antibody. B, BMMs were serum-starved for 5 h, pretreated with or without U0126 (0.1–10  $\mu\text{M}$ ) for 2 h, and stimulated with RANKL (500 ng/ml) for the indicated time. Phospho-ERK1/2 levels were determined by immunoblotting. C and D, BMMs were cultured in the osteoclastogenic medium for 3 days in the presence or absence of U0126 (0.1–10  $\mu\text{M}$ ). Cells were stained for TRAP (C), and TRAP<sup>+</sup> MNCs were counted (D). E, BMMs were incubated in medium containing M-CSF (30 ng/ml) or M-CSF plus RANKL (200 ng/ml) for 24 h with indicated dose of U0126 (0.1–10  $\mu\text{M}$ ). The whole cell lysates were analyzed by immunoblotting with anti-c-Fos and anti-NFATc1 antibodies.

activation by RANKL was not affected by LY294002 (Fig. 8B, third panel), demonstrating that PI3K/Akt is not an upstream target of DMS for the inhibition of ERK1/2 activation by RANKL. Furthermore, LY294002 inhibited the induction of c-Fos and NFATc1 by RANKL (Fig. 8C). These results are congruent with previous works indicating that the PI3K/Akt pathway is required for AP-1 activation through c-Fos expression (Huang et al., 1996). Therefore, it seems that Akt inhibition by DMS also contributes to the blockade of NFATc1 induction, independently of its ERK inhibition.

**Effect of c-Fos Overexpression on Osteoclastogenesis in DMS-Treated BMMs.** If the inhibition of RANKL-induced ERK/Akt activation and c-Fos expression is the critical cause of NFATc1 down-regulation, one would expect that the DMS-mediated inhibition of osteoclastogenesis would be overcome by ectopic c-Fos overexpression. Thus, we examined whether transient overexpression of c-Fos would recover osteoclastogenesis in the presence of DMS. BMMs were infected with recombinant retroviruses harboring GFP alone or GFP plus c-Fos. When the infection efficiency was evaluated by scoring GFP-positive cells, it was 80 to 90% (Fig. 9A). The overexpression of c-Fos was verified by Western blotting with anti-c-Fos (Fig. 9B). In cultures of c-Fos-overexpressing BMMs, there was a significant increase in TRAP<sup>+</sup> osteoclast numbers in the presence of DMS compared with the control virus-infected BMMs (Fig. 9, C and D). These data suggest

that c-Fos was a critical downstream target of DMS inhibition in the RANKL signaling for osteoclast differentiation.

## Discussion

During an approach to identify genes involved in the osteoclastogenesis using DNA microarrays, we found that SPHK1 expression was significantly increased upon RANKL treatment. SPHK has been implicated in the differentiation of various types of cells. In addition, the proinflammatory factors such as lipopolysaccharide and TNF- $\alpha$ , which augment RANKL-induced osteoclastogenesis, stimulate SPHK in macrophages and epithelial cells (Xia et al., 1999; Shu et al., 2002). These backgrounds led us to test the potential role of SPHK for the differentiation of precursor cells into mature osteoclasts. The function of SPHK is usually estimated in vitro studies by treating cells with DMS, a well established competitive inhibitor of SPHK (Igarashi and Hakomori, 1989). In the present study, treatment of osteoclast precursors with DMS resulted in an almost complete inhibition of RANKL-induced osteoclast differentiation. Considering that

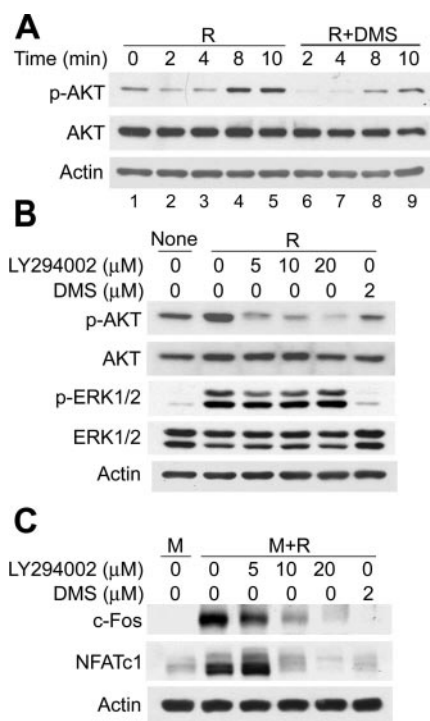


**Fig. 8.** DMS also inhibits the PI3K/Akt pathway. A, BMMs were serum-starved for 5 h, pretreated with or without DMS (2  $\mu$ M) for 2 h, and stimulated with RANKL (500 ng/ml) for the indicated time. Cell lysates were analyzed by immunoblotting for phospho-Akt or total Akt level. B, serum-starved BMMs were pretreated with indicated concentration of LY294002 (5–20  $\mu$ M) or DMS (2  $\mu$ M) for 2 h and stimulated with RANKL (500 ng/ml) for 5 min. Phosphorylation of Akt and ERK1/2 was analyzed by immunoblotting. C, BMMs were incubated in medium containing M-CSF (30 ng/ml) or M-CSF plus RANKL (200 ng/ml) for 24 h with indicated dose of LY294002 (5–20  $\mu$ M) or DMS (2  $\mu$ M). The whole-cell lysates were analyzed by immunoblotting with anti-c-Fos and anti-NFATc1 antibodies.

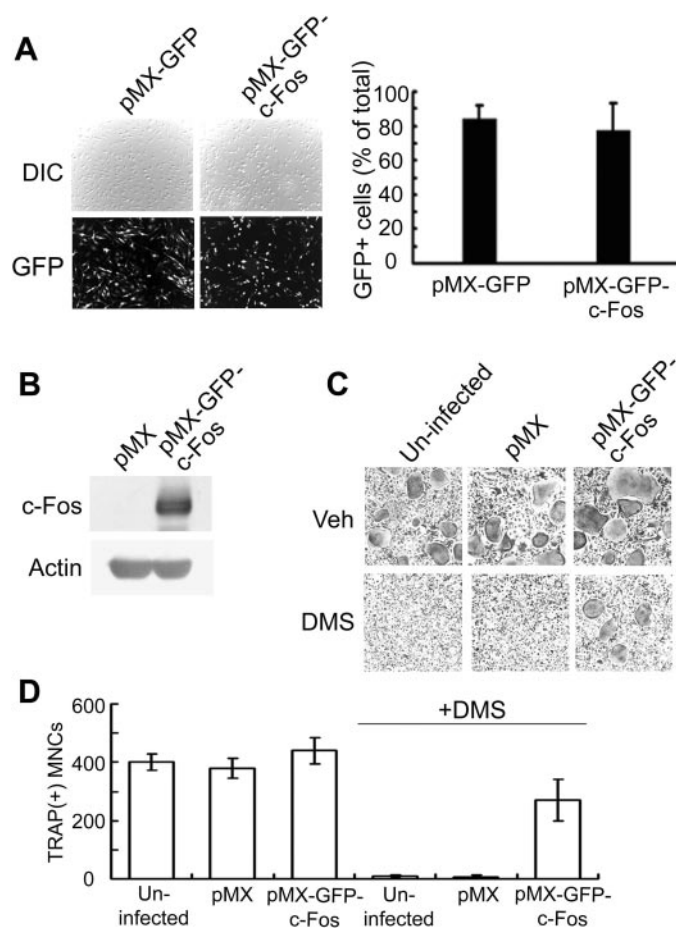


**Fig. 9.** c-Fos overexpression overcomes the antiosteoclastogenic effect of DMS. A, BMMs were infected with c-Fos or control retroviruses. At 24 h after infection, cells were subjected to fluorescence microscopy to examine the efficiency of infection. Representative pictures of infected cells are shown (left), and the percentage GFP<sup>+</sup> cells was quantified (right). B, infected BMMs were cultured for 24 h and cell extracts were analyzed for c-Fos expression levels by immunoblotting. C and D, BMMs uninfected or infected with either c-Fos or the control retroviruses were cultured in the osteoclastogenic medium for 3 days in the presence or absence of DMS (2  $\mu$ M). Cells were TRAP-stained (C) and TRAP<sup>+</sup> MNC numbers were counted (D).

the expression of SPHK was significantly increased upon RANKL treatment, the activity of SPHK might have been crucial for the RANKL-induced osteoclastogenesis. To test this possibility, SPHK in the osteoclast precursor BMMs were knocked down using a retroviral gene transfer system for siRNA. We were surprised to find that when these cells were stimulated to differentiate into osteoclasts by RANKL treatment, SPHK1 and SPHK2 siRNA-expressing cells generated a higher number of osteoclasts than the control siRNA-infected cells. Furthermore, DMS efficiently inhibited the RANKL-induced osteoclastogenesis in SPHK1-overexpressed BMMs. In line with these observations, exogenous addition of S1P to the culture medium could not recover osteoclast differentiation in the presence of DMS. In addition, we could not find antiosteoclastogenic effect using another inhibitor of SPHK, *DL-threo*-dihydrosphingosine. Taken together, these results indicate that DMS blocks RANKL-induced osteoclastogenesis independently of its SPHK inhibitory activity. We have previously suggested that SPHK1 and intracellular S1P may act as a negative feedback regulator during osteoclastogenesis (Ryu et al., 2006). On the other hand, secreted S1P stimulated osteoblast migration and survival, thus playing an osteoclast-osteoblast communication factor. The observation in this article that the siRNA against SPHK1/2 potentiated osteoclastogenesis further supports a negative role of SPHK during osteoclast differentiation. However, further studies are required to clearly delineate the role of SPHK during osteoclastogenesis in the context of cooperation with osteoblasts or T cells.

Because DMS was first reported as an inhibitor of protein kinase C (PKC) (Hannun and Bell, 1987), we considered the possibility of involvement of PKC pathways in the DMS-mediated osteoclastogenesis inhibition. It has been reported that the activation of PKC by 12-O-tetradecanoylphorbol-13-acetate inhibited osteoclastogenesis (Wang et al., 2003) and that a PKC-activating synthetic peptide fragment significantly decreased osteoclast activity (Moonga and Dempster, 1998). In our culture system, we could find no differences in PKC activation after the treatment of cells with DMS at concentrations that significantly inhibited osteoclastogenesis (data not shown). Moreover, the concentration of DMS required for PKC inhibitory effect is much higher than the DMS dose at which osteoclast differentiation was inhibited in our study (Edsall et al., 1998; Hamaguchi et al., 2003). Therefore, it is likely that PKC was not involved in DMS inhibition of osteoclastogenesis under our experimental conditions. Because it seemed that the SPHK and PKC were not involved, we tried to delineate the mechanism by which DMS exerts its inhibitory effect on RANKL-induced osteoclastogenesis. First, the effect of DMS on the expression of transcription factors crucially involved in the osteoclast differentiation was investigated. NFATc1 is the master transcription factor for osteoclastogenesis, and the distinguishing feature of NFATc1 induction by RANKL is its regulation by  $\text{Ca}^{2+}$  oscillation and c-Fos (Takayanagi et al., 2002). Controversial results have been reported concerning DMS, SPHK, and  $\text{Ca}^{2+}$  signals. It has been reported that DMS increases cytosolic calcium in human T lymphocytes (Alfonso et al., 2003) and monocytes (Lee et al., 2006). On the contrary, some studies have shown the opposite results. Melendez and Ibrahim (2004) showed that C5a-triggered cytosolic  $\text{Ca}^{2+}$  signals are inhibited by

DMS, and Yadav et al. (2006) demonstrated that SPHK mediates cytosolic  $\text{Ca}^{2+}$  increase upon mycobacterial infection in mouse BMMs. In our experiments, DMS had little effect on the RANKL-induced  $\text{Ca}^{2+}$  oscillation. On the other hand, enforced c-Fos expression reversed the DMS inhibition of osteoclastogenesis and restored NFATc1 expression, suggesting that c-Fos might be a critical downstream target of DMS for the inhibition of RANKL-induced osteoclastogenesis. The RANKL-induced phosphorylation and subsequent degradation of I $\kappa$ B and the RANKL-stimulated transcription activity of NF $\kappa$ B were not significantly affected by DMS treatment, suggesting that the inhibitory effects of DMS on osteoclast differentiation do not involve NF $\kappa$ B signaling pathway. Thus, the inhibition of osteoclastogenesis by DMS was mediated by controlling specific signaling pathways, not by cytotoxicity.

RANKL is known to activate three major MAPK subfamilies (ERK, JNK, and p38), and inhibition of these MAPKs suppresses osteoclast differentiation (Matsumoto et al., 2000; Boyle et al., 2003; Lee and Kim, 2003). We found that the effect of DMS on the RANKL-induced MAPK activation in BMMs was very selective; i.e., whereas the ERK activation was prominently inhibited by DMS, the activation of JNK and p38 was nearly unaffected. Because it was reported previously that the ERK1/2 activation led to the stimulation of c-Fos expression by acting on transcription factors bound at the c-Fos promoter in various cell types (Triesman, 1996; Müller et al., 1997), the involvement of ERK pathway signaling in the inhibition of osteoclastogenesis and c-Fos expression by DMS was investigated. The ERK upstream activators that have been mostly well characterized are MEK1/2. We found that DMS exerts inhibitory effects on the activation of MEK1/2 by RANKL in osteoclast precursor BMMs. When BMMs were treated with the MEK inhibitor U0126, these cells failed to differentiate into osteoclasts. Furthermore, U0126 had a similar inhibitory effect on the RANKL-induced c-Fos and NFATc1 expression. Although further study is required to fully define the direct molecular target for the

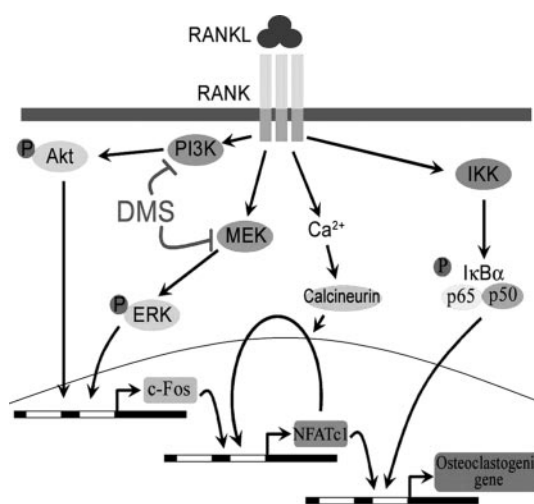


**Fig. 10.** A schematic model for the osteoclastogenesis inhibitory function of DMS. RANKL engagement to RANK results in the activation of both MEK/ERK and PI3K/Akt pathways. Combined inhibition of the two pathways by DMS significantly reduces the induction of c-Fos and NFATc1 transcription factors by RANKL. The blockade of these transcription factors leads to suppression of osteoclastogenic gene expression and subsequent osteoclast formation.

inhibition of MEK by DMS, it is clear that the inhibition of the MEK/ERK pathway, and subsequent hampering of the RANKL-stimulated c-Fos/NFATc1 expression is crucial for the antiosteoclastogenic effect of DMS.

In our study, DMS also significantly inhibited RANKL-induced Akt phosphorylation. PI3K has been shown to stimulate ERK1/2 activation in response to some stimuli (Grønning et al., 2002; Zhuang et al., 2004; Lee et al., 2005). Thus, the possibility that DMS inhibited ERK by reducing PI3K activity was tested by treating cells with the PI3K inhibitor LY294002. The inhibition of PI3K resulted in the reduction of RANKL-induced expression of c-Fos and NFATc1, which was also observed after DMS treatment. These results are congruent with those from previous works that have indicated PI3K activation to be required for c-Fos expression and AP-1 activation (Huang et al., 1996). However, LY294002 did not inhibit RANKL-induced ERK phosphorylation, indicating that these two pathways are distinct. Consistent with our data, Wilden et al. (1998) showed that smooth muscle cell proliferation requires independent ERK and PI3K activation, and Monick et al. (2004) demonstrated that DMS blocks, through separate mechanisms, the activation of both ERK and Akt upon viral infection in epithelial cells. Thus, DMS is likely to exert its antiosteoclastogenic effect through inhibitory action on the two separate signaling pathways crucial for RANKL-induced osteoclastogenesis (i.e., the MEK/ERK and the PI3K/Akt pathways) (Fig. 10).

The antiosteoclastogenic property of DMS may have very important clinical implications. Anticancer effects of DMS, such as inhibition of tumor cell growth and migration, have been reported, triggering intensive studies for application of DMS as an anticancer drug (Endo et al., 1991). It is noteworthy that patients with advanced breast and prostate cancers usually develop bone metastasis, because these cancer cells find bone to be a fertile soil in which to grow (Mundy, 2002). One of the cues that attract cancer cells to the bone is the bone-derived growth factors such as transforming growth factor  $\beta$ , insulin-like growth factor 1, and fibroblast growth factor, which are released during osteoclastic bone resorption. Consistent with this notion, it has been shown that osteoprotegerin, a natural antagonist of RANKL, inhibited bone metastasis in an animal model (Mundy, 2002). These findings suggest the possibility that osteolysis inhibitors might also decrease bone tumor burden. Thus, the anticancer properties previously reported and the antiosteoclastogenic activity shown in our present study mark DMS as a uniquely interesting drug candidate for treatment of tumor bone metastases. In summary, our study provides the first evidence that DMS suppresses osteoclastogenesis from primary precursors and points out the potential usefulness of this sphingolipid for the treatment of bone-associated tumors.

## References

- Alfonso A, De la Rosa LA, Veytes MR, and Botana LM (2003) Dimethylsphingosine increases cytosolic calcium and intracellular pH in human T lymphocytes. *Biochem Pharmacol* **65**:465–478.
- Boyle WJ, Simonet WS, and Lacey DL (2003) Osteoclast differentiation and activation. *Nature* **423**:337–342.
- Edsall LC, Van Brocklyn JR, Cuvillier O, Kleuser B, and Spiegel S (1998) *N,N*-Dimethylsphingosine is a potent competitive inhibitor of sphingosine kinase but not of protein kinase C: modulation of cellular levels of sphingosine 1-phosphate and ceramide. *Biochemistry* **37**:12892–12898.
- Endo K, Igarashi Y, Nisar M, Zhou QH, and Hakomori S (1991) Cell membrane signaling as target in cancer therapy: inhibitory effect of *N,N*-dimethyl and *N,N,N*-trimethyl sphingosine derivatives on in vitro and in vivo growth of human tumor cells in nude mice. *Cancer Res* **51**:1613–1618.
- Grønning LM, Cederberg A, Miura N, Enerback S, and Tasken K (2002) Insulin and TNF- $\alpha$  induce expression of the Forkhead transcription factor gene Foxc2 in 3T3-L1 adipocytes via PI3K and ERK1/2-dependent pathway. *Mol Endocrinol* **16**:873–883.
- Ha H, Kwak HB, Lee SK, Na DS, Rudd CE, Lee ZH, and Kim HH (2003) Membrane rafts play a crucial role in receptor activator of nuclear factor kappaB signaling and osteoclast function. *J Biol Chem* **278**:18573–18580.
- Hamaguchi A, Suzuki E, Murayama K, Fujimura T, Hikita T, Iwabuchi K, Handa K, Withers DA, Masters SC, Fu H, et al. (2003) Sphingosine-dependent protein kinase-1, directed to 14–3-3, is identified as the kinase domain of protein kinase C delta. *J Biol Chem* **278**:41557–41565.
- Hannun YA and Bell RM (1987) Lysosphingolipids inhibit protein kinase C: implication for the sphingolipidoses. *Science* **235**:670–674.
- Huang C, Ma WY, and Dong Z (1996) Requirement for phosphatidylinositol 3-kinase in epidermal growth factor-induced AP-1 transactivation and transformation in JB6 P+ cells. *Mol Cell Biol* **16**:6427–6435.
- Huang H, Ryu J, Ha J, Chang EJ, Kim HJ, Kim HM, Kitamura T, Lee ZH, and Kim HH (2006) Osteoclast differentiation requires TAK1 and MKK6 for NFATc1 induction and NF- $\kappa$ B transactivation by RANKL. *Cell Death Differ* **13**:1879–1891.
- Igarashi Y and Hakomori S (1989) Enzymatic synthesis of *N,N*-dimethylsphingosine: demonstration of the sphingosine:*N*-methyltransferase in mouse brain. *Biochem Biophys Res Commun* **164**:1411–1416.
- Kohama T, Olivera A, Edsall L, Nagiec MM, Dickson R, and Spiegel S (1998) Molecular cloning and functional characterization of murine sphingosine kinase. *J Biol Chem* **273**:23722–23728.
- Lee C, Tomkowicz B, Freedman BD, and Collman RG (2005) HIV-1 gp120-induced TNF- $\alpha$  production by primary human macrophages is mediated by phosphatidylinositol-3 (PI-3) kinase and mitogen-activated protein (MAP) kinase pathway. *J Leukocyte Biol* **78**:1016–1023.
- Lee EH, Lee YK, Im YJ, Kim JH, Okajima F, and Im DS (2006) Dimethylsphingosine regulates intracellular pH and  $\text{Ca}^{2+}$  in human monocytes. *J Pharmacol Sci* **100**:289–296.
- Lee ZH and Kim HH (2003) Signal transduction by receptor activator of nuclear factor kappa B in osteoclasts. *Biochem Biophys Res Commun* **305**:211–214.
- Matsumoto M, Sudo T, Saito T, Osada H, and Tsujimoto M (2000) Involvement of p38 mitogen-activated protein kinase signaling pathway in osteoclastogenesis mediated by receptor activator of NF- $\kappa$ B ligand (RANKL). *J Biol Chem* **275**:31155–31161.
- Matsuo K and Ray N (2004) Osteoclasts, mononuclear phagocytes, and c-Fos: new insight into osteoimmunology. *Keio J Med* **53**:78–84.
- Matsuo K, Galson DL, Zhao C, Peng L, Laplace C, Wang KZ, Bachler MA, Amano H, Aburatani H, Ishikawa H, et al. (2004) Nuclear factor of activated T-cells (NFAT) rescues osteoclastogenesis in precursors lacking c-Fos. *J Biol Chem* **279**:26475–26480.
- Melendez AJ and Ibrahim FB (2004) Antisense knockdown of sphingosine kinase 1 in human macrophages inhibits C5a receptor-dependent signal transduction,  $\text{Ca}^{2+}$  signals, enzyme release, cytokine production, and chemotaxis. *J Immunol* **173**:1596–1603.
- Monick MM, Cameron K, Powers LS, Butler NS, McCoy D, Mallampalli RK, and Hunninghake GW (2004) Sphingosine kinase mediates activation of extracellular signal-related kinase and Akt by respiratory syncytial virus. *Am J Respir Cell Mol Biol* **30**:844–852.
- Moonga BS and Dempster DW (1998) Effects of peptide fragments of protein kinase C on isolated rat osteoclasts. *Exp Physiol* **83**:717–725.
- Müller JM, Krauss B, Kaltschmidt C, Baeuerle PA, and Rupec RA (1997) Hypoxia induces c-Fos transcription via a mitogen-activated protein kinase-dependent pathway. *J Biol Chem* **272**:23435–23439.
- Mundy GR (2002) Metastasis to bone: causes, consequences and therapeutic opportunities. *Nat Rev Cancer* **2**:584–593.
- Olivera A and Spiegel S (1993) Sphingosine-1-phosphate as second messenger in cell proliferation induced by PDGF and FCS mitogens. *Nature* **365**:557–560.
- Payne DM, Rossomando AJ, Martino P, Erikson AK, Her JH, Shabanowitz J, Hunt DF, Weber MJ, and Sturgill TW (1991) Identification of the regulatory phosphorylation sites in pp42/mitogen-activated protein kinase (MAP kinase). *EMBO J* **10**:885–892.
- Pearson G, Robinson F, Gibson TB, Xu B, Karandikar M, Berman K, and Cobb MH (2001) Mitogen-activated protein kinase pathway: regulation and physiological functions. *Endocr Rev* **22**:153–183.
- Ryu J, Kim HJ, Chang EJ, Huang H, Banno Y, and Kim HH (2006) Sphingosine 1-phosphate as a regulator of osteoclast differentiation and osteoclast-osteoblast coupling. *EMBO J* **25**:5840–5851.
- Shu X, Wu W, Mosteller RD, and Broek D (2002) Sphingosine kinase mediates vascular endothelial growth factor-induced activation of Ras and mitogen-activated protein kinases. *Mol Cell Biol* **22**:7758–7768.
- Spiegel S and Milstien S (2003) Sphingosine-1-phosphate: an enigmatic signaling lipid. *Nat Rev Mol Cell Biol* **4**:397–407.
- Takatsuna H, Asagiri M, Kubota T, Oka K, Osada T, Sugiyama C, Sato H, Aoki K, Ohya K, Takayanagi H, et al. (2005) Inhibition of RANKL-induced osteoclastogenesis by (-)-DHMEQ, a novel NF- $\kappa$ B inhibitor, through downregulation of NFATc1. *J Bone Miner Res* **20**:653–662.
- Takayanagi H, Kim S, Koga T, Nishina H, Isshiki M, Yoshida H, Saiura A, Isobe M, Yokochi T, Inoue J, et al. (2002) Induction and activation of the transcription factor NFATc1 (NFAT2) integrate RANKL signaling in terminal differentiation of osteoclasts. *Dev Cell* **3**:889–901.
- Tauzin L, Graf C, Sun M, Rovina P, Bouveyron N, Jaritz M, Winiski A, Hartmann N, Staedtler F, Billich A, et al. (2007) Effects of ceramide-1-phosphate on cultured cells: dependence on dodecane in the vehicle. *J Lipid Res* **48**:66–76.
- Teitelbaum SL (2004) RANKing c-Jun in osteoclast development. *J Clin Invest* **114**:463–465.

- Treisman R (1996) Regulation of transcription by MAP kinase cascades. *Curr Opin Cell Biol* **8**:205–215.
- Walsh MC, Kim N, Kadono Y, Rho J, Lee SY, Lorenzo J, and Choi Y (2006) Osteoimmunology: interplay between the immune system and bone metabolism. *Annu Rev Immunol* **24**:33–63.
- Wang C, Steer JH, Joyce DA, Yip KH, Zheng MH, and Xu J (2003) 12-*O*-tetradecanoylphorbol-13-acetate (TPA) inhibits osteoclastogenesis by suppressing RANKL-induced NF- $\kappa$ B activation. *J Bone Miner Res* **18**:2159–2168.
- Wei S, Wang MW, Teitelbaum SL, and Ross FP (2002) Interleukin-4 reversibly inhibits osteoclastogenesis via inhibition of NF- $\kappa$ B and mitogen-activated protein kinase signaling. *J Biol Chem* **277**:6622–6630.
- Wilden PA, Agazie YM, Kaufman R, and Halenda SP (1998) ATP-stimulated smooth muscle cell proliferation requires independent ERK and PI3K signaling pathways. *Am J Physiol* **275**:H1209–H1215.
- Wong BR, Besser D, Kim N, Arron JR, Vologodskaya M, Hanafusa H, and Choi Y (1999) TRANCE, a TNF family member, activates Akt/PKB through a signaling complex involving TRAF6 and c-Src. *Mol Cell* **4**:1041–1049.
- Wu W, Mosteller RD, and Broek D (2004) Sphingosine kinase protects lipopolysaccharide-activated macrophages from apoptosis. *Mol Cell Biol* **24**:7359–7369.
- Xia P, Wang L, Gamble JR, and Vadas MA (1999) Activation of sphingosine kinase by tumor necrosis factor- $\alpha$  inhibits apoptosis in human endothelial cells. *J Biol Chem* **274**:34499–34505.
- Yadav M, Clark L, and Schorey JS (2006) Macrophage's proinflammatory response to a mycobacterial infection is dependent on sphingosine kinase-mediated activation of phosphatidylinositol phospholipase C, protein kinase C, ERK1/2, and phosphatidylinositol 3-kinase. *J Immunol* **176**:5494–5503.
- Zhuang ZY, Xu H, Clapham DE, and Ji RR (2004) Phosphatidylinositol 3-kinase activates ERK in primary sensory neurons and mediates inflammatory heat hyperalgesia through TRPV1 sensitization. *J Neurosci* **24**:8300–8309.

---

**Address correspondence to:** Hong-Hee Kim, Department of Cell and Developmental Biology, Seoul National University, 28 Yeongon-Dong, Chongno-Gu, Seoul 110-749, Korea. E-mail: hhbkim@snu.ac.kr

---